Published for SISSA by Springer

Received: *August 18, 2022*
Accepted: *October 13, 2022*
Published: *October 25, 2022*

Complete SMEFT predictions for four top quark production at hadron colliders

Rafael Aoude,[a] **Hesham El Faham,**[a,b] **Fabio Maltoni**[a,c] **and Eleni Vryonidou**[d]

[a] *Centre for Cosmology, Particle Physics and Phenomenology (CP3), Université Catholique de Louvain, Chemin du Cyclotron, B-1348 Louvain la Neuve, Belgium*
[b] *Inter-University Institute for High Energies (IIHE), Vrije Universiteit Brussel, Pleinlaan 2, 1050 Brussels, Belgium*
[c] *Dipartimento di Fisica e Astronomia, Università di Bologna and INFN, Sezione di Bologna, Via Irnerio 46, 40126 Bologna, Italy*
[d] *Department of Physics and Astronomy, University of Manchester, Oxford Road, Manchester M13 9PL, U.K.*

E-mail: rafael.aoude@uclouvain.be, hesham.el.faham@vub.be, fabio.maltoni@uclouvain.be, eleni.vryonidou@manchester.ac.uk

Abstract: We study four top quark production at hadron colliders in the Standard Model Effective Field Theory (SMEFT). We perform an analysis at the tree-level, including all possible QCD- and EW-coupling orders and relevant dimension-six operators. We find several cases where formally subleading terms give rise to significant contributions, potentially providing sensitivity to a broad class of operators. Inclusive and differential predictions are presented for the LHC and a future *pp* circular collider operating at 100 TeV. We estimate the sensitivity of different operators and perform a simplified chi-square fit to set limits on SMEFT Wilson coefficients. In so doing, we assess the importance of including subleading terms and differential information in constraining new physics contributions. Finally, we compute the SMEFT predictions for the double insertion of dimension-six operators and scrutinise the possible enhancements to the sensitivity induced by a specific class of higher order terms in the EFT series.

Keywords: Higher Order Electroweak Calculations, SMEFT

ArXiv ePrint: 2208.04962

https://doi.org/10.1007/JHEP10(2022)163

JHEP10(2022)163

Contents

JHEP10(2022)163

1 Introduction

In the last decade, the Large Hadron Collider (LHC) experiment at CERN has tested our understanding of fundamental interactions up to several TeV's of energy. The unexpected success of the Standard Model (SM), on the one hand, and its inherent incompleteness as a theory of nature, on the other hand, have led to vigorous efforts by the experimental and theoretical communities to study where new physics could lurk. In this endeavour, a unique role is played by precision physics, where accurate theoretical predictions of SM processes are compared with experimental measurements searching for deviations. The upcoming third run of the LHC — characterised by a 4.5% increase in collision centre of mass-energy, from 13 TeV to 13.6 TeV and a two-fold increase of luminosity- will provide a new handle on rare phenomena (for a review of the latest experimental measurements of $t\bar{t}t\bar{t}$ and future prospects at the LHC, see ref. [1]). Among the rarest and most spectacular processes at the LHC is the production of two pairs of top-antitop quarks, i.e., four top quark production. This process is characterised by a tiny SM cross-section at 13 TeV, of about 12 fb [2], i.e., around five orders of magnitude lower than that of $t\bar{t}$ production. However, despite the tiny rates, $t\bar{t}t\bar{t}$ signatures are distinctive, leading to a wealthy and energetic final state,

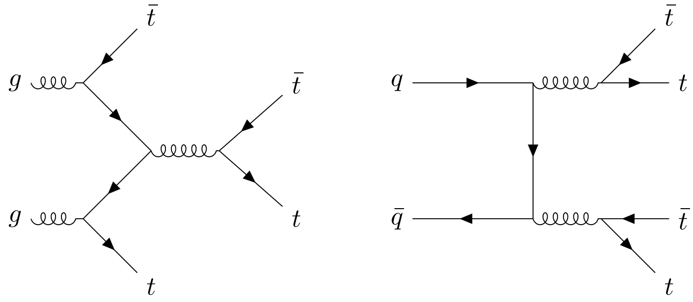

Figure 1. Representative leading order tree-level Feynman diagrams of $\mathcal{O}(\alpha_s^2)$ for the gg-initiated (*left*) and the $q\bar{q}$-initiated (*right*) SM four-top production at the LHC.

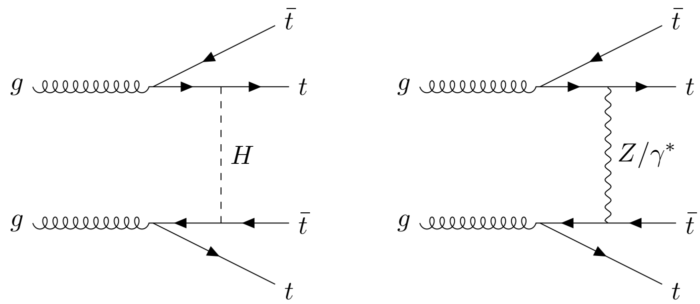

Figure 2. Representative diagrams of $\mathcal{O}(\alpha_s\alpha_{\rm w})$ for the SM four-top production at the LHC. The diagrams show the EW $tt \to tt$ scattering involving the exchange of a Higgs boson (*left*) or a Z-boson/virtual photon (*right*).

which is challenging to mimic through other processes. Therefore, the very high-Q^2 and low backgrounds offer a unique opportunity for probing new physics [3–17].

Given its promise, precise predictions of four-top production have become necessary. Next-to-leading order (NLO) corrections in QCD have been computed first in ref. [18] and then also become available in event generators [19–21]. The complete NLO predictions, including all possible QCD and electroweak (EW) orders, have been calculated in ref. [2]. They revealed a peculiar and unexpected interplay between EW and QCD contributions, with significant contributions with opposite signs arising from formally subleading terms. Significant subleading contributions have also been observed in the case of new physics contributions to four-top production [15, 22]. Moreover, it has been suggested in the study of ref. [23] that four-top production may be a valuable probe of the top-Yukawa coupling, y_t, at the tree-level.

In the SM, representative diagrams of the pure-QCD $\mathcal{O}(\alpha_s^2)$ four-top production are shown in figure 1, occurring through gg and $q\bar{q}$ initial states. QCD-induced diagrams typically provide the leading contribution. However, formally subleading diagrams with insertions of EW couplings, i.e. $\mathcal{O}(\alpha_s\alpha_{\rm w})$, can also be significant. Examples of the latter are shown in figure 2, where top quarks scatter through the exchange of a Higgs boson or Z/γ^*. These diagrams can contribute through their interference with QCD ones or through their squares. In the SM at $\sqrt{s} = 13\,\text{TeV}$, it turns out that contributions from the inter-

JHEP10(2022)163

ference of this class of diagrams with the leading QCD amplitude and from their squares are significant, reaching more than a third of the leading tree-level QCD contributions. Nevertheless, these two contributions come with opposite signs, and there is a significant cancellation between them. This can be seen explicitly in table 7 of ref. [2]. These large cancellations at the tree-level also motivate a high-order computation, including QCD and EW corrections, as discussed in ref. [2]. At one-loop order, additional cancellations occur between different terms in the α_s and α_{w} expansion, but in general, higher-order corrections are dominated by α_s corrections to the leading QCD term. It is worth noting that the size of various terms varies significantly depending on the choice of the renormalisation scale. Though it is clear from table 7 of ref. [2] that several contributions are larger than what one would expect from the ratio of $\alpha_{\mathrm{w}}/\alpha_s$. In summary, four-top production does not necessarily submit to the "naive" α_s and α_{w} power counting. Therefore, a study of four-top production should be completed by including all QCD and EW-induced terms in the computations. This consideration constitutes the primary motivation behind the work presented in this paper.

The peculiar behaviour of the cross-section as a double series in α_s and α_{w} for the SM process certainly motivates a detailed study in the case of including new physics effects, particularly in the SMEFT framework. The effective field theory approach assumes new physics to reside at a high scale Λ [24–26]. In the SMEFT, the SM Lagrangian is augmented with higher-dimensions operators built out of the SM fields and respecting the SM gauge symmetries, describing short-distance interactions generated by new physics at high scales. The pattern of such deformation depends on the details of the phenomena in the ultra-violet (UV) region. Being unknown, one assumes all possible operators to be there and studies their effects on low-energy observables. The beauty of this framework is that it allows perturbative calculations to be performed consistently order by order in the $1/\Lambda$ expansion. Such a powerful approach provides a consistent and calculable framework in which the potential deviations from the SM predictions can be encapsulated and predicted in type and pattern. Studies in the context of the SMEFT at the LHC are an ongoing effort in all SM sectors; the electroweak, the Higgs, the flavour, and the top sectors. Global fits combining a broad set of publicly available data have appeared [27–32], indicating which directions (operators) in the fits can be constrained and whether complementary information or new strategies would be helpful. In the context of an EFT, four-top production is exciting as it is the simplest process where top quark self-interactions could be probed at the tree-level. In the SMEFT language, such interactions are described by a set of dimension-six operators of the form $\bar{\psi}\psi\bar{\psi}\psi$ operators with four top quark fields (left- or right-handed). Other processes at colliders do not directly constrain these operators at the tree-level. Therefore four-top production is naively expected to be the first place to see their effects.[1]

This work considers all possible contributions of the SM and the SMEFT, including all the dimension-six CP-even SMEFT operators that enter at the tree-level. Part of our motivation is that in the SMEFT, the EFT interference with the SM is expected to provide the leading cross-section contribution. As the interference projects the kinematic and the

[1]Proposals for constraining four-top operators through loop effects have appeared in refs. [16, 22, 33, 34].

colour structure of the SM amplitudes, its size can change significantly from one operator to another. It is also expected to vary depending on which contributions are included in the SM, as different operators have different colour and chirality structures. As mentioned previously, we retain all possible tree-level contributions at different orders in QCD and EW couplings in our computations. Specifically, we split the EW-induced contributions into the gauge and top-Yukawa ones and determine the inclusive and differential predictions for the LHC and FCC-hh. We organise our predictions as an expansion in α_s, where each term is expanded in the weak parameters, highlighting the potential significance of the formally subleading terms.

To assess the reach of constraining the SMEFT Wilson coefficients (WCs) at future colliders, we perform (i) a signal-strength-based projection study for each operator at different collider energies obtaining theoretical limits on the corresponding WCs; (ii) simplified chi-square (χ^2) fits at different collider energies on selected sets of operators. In the latter case, we also include differential information and assess its constraining power compared to using only inclusive measurements.

Finally, we scrutinise the claim of ref. [35] on the enhanced EFT sensitivity of four-top production to 2-heavy-2-light four-fermion operators due to the contributions from double insertion. In ref. [35], it was argued that though formally equivalent to single dimension-eight insertions, in some UV models, double insertion could provide the dominant terms and four-top production could compete with much more abundant top quark pair production processes through enhancements scaling as $\sim (cE^2/\Lambda^2)^4$.

This paper is structured as follows: in section 2, we describe the theoretical tools for four-top production within the SMEFT framework, presenting the operators' definitions and the cross-section expansion in QCD and EW couplings. The inclusive and differential predictions are presented in section 3 and section 4, respectively. The signal-strength projection study and the χ^2 fits are presented in section 5 and section 6, respectively. We discuss the results from the cross-section computation considering double EFT insertions in section 7. The work is summarised and concluded in section 8.

2 SMEFT framework to four top quark production

2.1 Operators definitions

We compute the SMEFT contributions to four-top production using a specific flavour assumption which singles out the top quark interactions,

$$\mathrm{U}(3)_l \times \mathrm{U}(3)_e \times \mathrm{U}(2)_q \times \mathrm{U}(2)_u \times \mathrm{U}(3)_d \equiv \mathrm{U}(2)^2 \times \mathrm{U}(3)^3, \tag{2.1}$$

where the subscripts refer to the five-fermion representations of the SM. This minimal relaxation of the $\mathrm{U}(3)^5$ group gives rise to top quark chirality-flipping interactions, such as the dipole interactions and ones which modify the top-Yukawa coupling. We use the notation and operator conventions of refs. [22, 36] and study all operators in three classes of dimension-six SMEFT: four-fermion (4F), two-fermion (2F), and purely-bosonic (0F) operators, consistent with our flavour symmetry assumption. We do not consider the

JHEP10(2022)163

two-fermion light quark operators as we expect them to be better constrained in other production processes.

Four-fermion operators. Following the conventions and notation of ref. [36], the four-fermion operators are defined as follows:

$$\begin{aligned}
\mathcal{Q}_{qq}^{1(ijkl)} &= (\bar{q}_i\gamma^\mu q_j)(\bar{q}_k\gamma_\mu q_l), & \mathcal{Q}_{qq}^{3(ijkl)} &= (\bar{q}_i\gamma^\mu \tau^I q_j)(\bar{q}_k\gamma_\mu \tau^I q_l),\\
\mathcal{Q}_{qu}^{1(ijkl)} &= (\bar{q}_i\gamma^\mu q_j)(\bar{u}_k\gamma_\mu u_l), & \mathcal{Q}_{qu}^{8(ijkl)} &= (\bar{q}_i\gamma^\mu T^A q_j)(\bar{u}_k\gamma_\mu T^A u_l),\\
\mathcal{Q}_{qd}^{1(ijkl)} &= (\bar{q}_i\gamma^\mu q_j)(\bar{d}_k\gamma_\mu d_l), & \mathcal{Q}_{qd}^{8(ijkl)} &= (\bar{q}_i\gamma^\mu T^A q_j)(\bar{d}_k\gamma_\mu T^A d_l),\\
\mathcal{Q}_{ud}^{1(ijkl)} &= (\bar{u}_i\gamma^\mu u_j)(\bar{d}_k\gamma_\mu d_l), & \mathcal{Q}_{ud}^{8(ijkl)} &= (\bar{u}_i\gamma^\mu T^A u_j)(\bar{d}_k\gamma_\mu T^A d_l),\\
{}^\dagger\mathcal{Q}_{quqd}^{1(ijkl)} &= (\bar{q}_i u_j)\epsilon(\bar{q}_k d_l), & {}^\dagger\mathcal{Q}_{quqd}^{8(ijkl)} &= (\bar{q}_i T^A u_j)\epsilon(\bar{q}_k T^A d_l),\\
& & \mathcal{Q}_{uu}^{(ijkl)} &= (\bar{u}_i\gamma^\mu u_j)(\bar{u}_k\gamma_\mu u_l),
\end{aligned} \tag{2.2}$$

where the notation $\mathcal{Q}$ indicates operators are given in the original Warsaw basis [37]. In this work however, we use operators aligned with the `SMEFTatNLO` [22] conventions, hereafter referred to as the "top-basis" and denoted by $\mathcal{O}$. The difference lies in the slight modification of the four-fermion operators rendering them more suitable for top quark physics, as well as normalising the operators $\mathcal{O}_{tG}$ and $\mathcal{O}_G$ through the inclusion of an extra g_s factor in their definitions. The consequences of the latter normalisation are later discussed when presenting the inclusive predictions in section 3. The translations of all four-fermion operators from the Warsaw basis to the top-basis are given in table 5 of section A. We also present the recent constraints on their corresponding coefficients in table 6 of the same appendix based on the global analysis of ref. [29].

Two-fermion and purely-bosonic operators. The set of potentially relevant two-fermion operators to four-top production are defined as follows:

$$\begin{aligned}
\mathcal{Q}_{tB} &= i(\bar{Q}\tau^{\mu\nu}\, t)\,\tilde{\varphi}\, B_{\mu\nu} + \text{h.c.}, & \mathcal{O}_{t\varphi} &= (\varphi^\dagger\varphi - v^2/2)\bar{Q}t\tilde{\varphi} + \text{h.c.},\\
\mathcal{O}_{tW} &= i(\bar{Q}\tau^{\mu\nu}\,\tau_I\, t)\,\tilde{\varphi}\, W^I_{\mu\nu} + \text{h.c.}, & \mathcal{O}_{\varphi t} &= i(\varphi^\dagger \overset{\leftrightarrow}{D}_\mu\, \varphi)(\bar{t}\,\gamma^\mu\, t),\\
\mathcal{O}_{tG} &= ig_S\,(\bar{Q}\tau^{\mu\nu}\, T_A\, t)\,\tilde{\varphi}\, G^A_{\mu\nu} + \text{h.c.}, & \mathcal{Q}_{\varphi Q}^{(1)} &= i(\varphi^\dagger \overset{\leftrightarrow}{D}_\mu\, \varphi)(\bar{Q}\,\gamma^\mu\, Q),\\
& & \mathcal{Q}_{\varphi Q}^{(3)} &= i(\varphi^\dagger \overset{\leftrightarrow}{D}_\mu\, \tau_I\, \varphi)(\bar{Q}\,\gamma^\mu\, \tau^I\, Q).
\end{aligned} \tag{2.3}$$

For convenience and following the conventions of [22, 36] we consider the following linear combinations of Warsaw operators' coefficients:

$$c_{tW} = C_{tW},\; c_{tZ} = -\sin\theta_{\text{w}} C_{tB} + \cos\theta_{\text{w}} C_{tW}, \tag{2.4}$$

where we kept the notation c_i for coefficients of operators written in the top-basis while C_i denotes coefficients in Warsaw basis. Similarly, we use the linear combination $c_{\varphi Q}^{(-)} = C_{\varphi Q}^{(1)} - C_{\varphi Q}^{(3)}$ instead of the singlet piece (this combination is notated as `cpQM` in `SMEFTatNLO` while the triplet $c_{\varphi Q}^{(3)}$ as `cpQ3`). The coefficient $c_{\varphi Q}^{(3)}$ is irrelevant to four-top production since it modifies the tWb vertex.

On the other hand, the relevant purely-bosonic operators in the top-basis are defined as follows:

$$\mathcal{O}_{\varphi G} = \left(\varphi^\dagger\varphi - \frac{v^2}{2}\right) G_A^{\mu\nu} G_{\mu\nu}^A, \qquad \mathcal{O}_G = g_s f_{ABC} G_{\mu\nu}^A G^{B,\nu\rho} G_\rho^{C,\mu}. \tag{2.5}$$

The latter is constrained by studies including multi-jet production [38, 39]. Bounds on the $\mathcal{O}_{\varphi G}$ coefficient, as well as all two-fermion coefficients in eq. (2.3), are given in table 7 of section A. Operators that modify the Higgs couplings to the gauge bosons and those that enter via fields' redefinition have negligible contributions in four-top production. Therefore, we omit them in what follows as we expect them to be constrained much better in other processes.

Having defined the potential operators relevant to four-top production, we now move to analyse the SM and EFT amplitudes in orders of QCD and EW couplings and subsequently examine different terms contributing to the cross-section.

2.2 Leading order coupling expansion

In the presence of SMEFT operators, a generic scattering amplitude expanded in the $1/\Lambda$ parameter can be written as follows:

$$\mathcal{A} = \mathcal{A}_{\text{SM}} + \frac{1}{\Lambda^2}\mathcal{A}_{(\text{d6})} + \frac{1}{\Lambda^4}\left(\mathcal{A}_{(\text{d6})^2} + \mathcal{A}_{(\text{d8})}\right), \tag{2.6}$$

leading to the decomposition of the partonic differential cross-section up to $\mathscr{O}(\Lambda^{-4})$,

$$d\sigma = d\sigma_{\text{SM}} + \frac{1}{\Lambda^2} d\sigma_{\text{int}} + \frac{1}{\Lambda^4}\left(d\sigma_{\text{quad}} + d\sigma_{\text{dbl}} + d\sigma_{\text{d8}}\right). \tag{2.7}$$

The leading SMEFT contribution, $d\sigma_{\text{int}}$, arises as the linear interference between $\mathcal{A}_{\text{SM}}$ and $\mathcal{A}_{(\text{d6})}$, while the $d\sigma_{\text{quad}}$ and $d\sigma_{\text{dbl}}$ are the squared single-insertion (also known as the quadratic), and double-insertion contributions, respectively. All the $\mathscr{O}(\Lambda^{-4})$ contributions can be schematically written in terms of the amplitudes,

$$d\sigma_{\text{quad}} \sim |\mathcal{A}_{(\text{d6})}|^2, \qquad d\sigma_{\text{dbl}} \sim |\mathcal{A}_{\text{SM}}\,\mathcal{A}_{(\text{d6})^2}|, \qquad d\sigma_{\text{d8}} \sim |\mathcal{A}_{\text{SM}}\,\mathcal{A}_{(\text{d8})}|, \tag{2.8}$$

where the latter is the contribution arising from amplitudes with a single insertion of a dimension-eight operator interfering with the SM ones. The construction of the SMEFT dimension-eight basis was explored in [40, 41], however, the systematic treatment of those operators is beyond the scope of this work. In this work, we study all the contributions arising from dimension-six operators, including the particular case for which we examine the double-insertion ones, $d\sigma_{\text{dbl}}$, in section 7.

The SM differential cross-section can be expanded in orders of the QCD and EW couplings,

$$d\sigma_{\text{SM}} = \sum_{n,m} \alpha_s^n\, \alpha_{\text{w}}^m\, d\sigma_{\text{SM}}^{(n,m)} = \sum_{i,j,k} \alpha_s^i\, \alpha^j\, \alpha_t^k\, d\sigma_{\text{SM}}^{(i,j,k)}, \tag{2.9}$$

JHEP10(2022)163

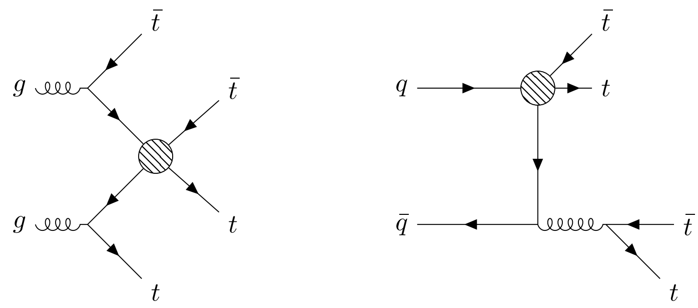

Figure 3. Representative diagrams for four-top production with blobs representing the one dimension-six EFT insertion, in the gg-initiated production mode (*left*) and in the $q\bar{q}$-initiated production mode (*right*).

JHEP10(2022)163

with $\alpha_{\rm w}$ collectively representing α and α_t, and

$$\alpha_s = \frac{g_s^2}{4\pi}, \qquad \alpha = \frac{e^2}{4\pi}, \qquad \alpha_t = \frac{y_t^2}{4\pi}. \tag{2.10}$$

The four-top production occurs via the $gg-$ and $q\bar{q}$-initiated channels. Each of the amplitudes is a six-point diagram and thus has four couplings, i.e. $(i + j + k) = 2$, and so we expand the $gg-$ and $q\bar{q}$-initiated SM amplitudes in terms of the QCD and EW couplings as follows:

$$\mathcal{A}^{(i,j,k)}_{\mathrm{SM},gg} = \alpha_s^2\, \mathcal{A}^{(2,0,0)}_{\mathrm{SM},gg} + \alpha_s \left(\alpha\, \mathcal{A}^{(1,1,0)}_{\mathrm{SM},gg} + \alpha_t\, \mathcal{A}^{(1,0,1)}_{\mathrm{SM},gg} \right), \tag{2.11a}$$

$$\begin{aligned} \mathcal{A}^{(i,j,k)}_{\mathrm{SM},qq} &= \alpha_s^2\, \mathcal{A}^{(2,0,0)}_{\mathrm{SM},qq} + \alpha_s \left(\alpha\, \mathcal{A}^{(1,1,0)}_{\mathrm{SM},qq} + \alpha_t\, \mathcal{A}^{(1,0,1)}_{\mathrm{SM},qq} \right) \\ &\quad + \left(\alpha^2\, \mathcal{A}^{(0,2,0)}_{\mathrm{SM},qq} + \alpha^{3/2}\, \alpha_t^{1/2}\, \mathcal{A}^{(0,3/2,1/2)}_{\mathrm{SM},qq} + \alpha\, \alpha_t\, \mathcal{A}^{(0,1,1)}_{\mathrm{SM},qq} \right), \end{aligned} \tag{2.11b}$$

with the term containing half-integer couplings, i.e. $\mathscr{O}(\alpha^{3/2}\, \alpha_t^{1/2})$, arising from diagrams containing a Higgs boson coupling to a top quark via one top-Yukawa vertex and a coupling to two EW bosons via one EW vertex. Each of the two W bosons couples with a fermion line.

Moving to the EFT case, as an example, we show the cross-section expansion for one class of operators; the four-fermion ones. The insertions of a single dimension-six four-fermion operator in the amplitudes of both production channels are depicted in figure 3. The EFT linear interference cross-section can be decomposed in the same way as the SM,

$$d\sigma_{\mathrm{int}} = \sum_{n,m} \alpha_s^n\, \alpha_{\rm w}^m\, d\sigma^{(n,m)}_{\mathrm{int}} = \sum_{i,j,k} \alpha_s^i\, \alpha^j\, \alpha_t^k\, d\sigma^{(i,j,k)}_{\mathrm{int}}, \tag{2.12}$$

where each of the expanded partial cross-section is a sum of contributions from different WCs,

$$d\sigma^{(n,m)}_{\mathrm{int}} = c_{[r]} d\sigma^{(n,m)}_{\mathrm{int}\,[r]}. \tag{2.13}$$

The index $[r]$ runs over all possible dimension-six operators. For the discussion, we write the EFT linear interference cross-section in terms of the SM and EFT amplitudes,

$$d\sigma_{\mathrm{int}} = d\sigma_{\mathrm{int},gg} + d\sigma_{\mathrm{int},qq} \sim 2\Re \left(\mathcal{A}_{\mathrm{SM},gg}\, \mathcal{A}^{\dagger}_{\mathrm{EFT},gg} \right) + 2\Re \left(\mathcal{A}_{\mathrm{SM},qq}\, \mathcal{A}^{\dagger}_{\mathrm{EFT},qq} \right), \tag{2.14}$$

(we have omitted the PDF dependence for simplicity) with the four-fermion EFT amplitudes reading

$$\mathcal{A}^{(i,j,k)}_{\text{EFT},gg,[\texttt{4F}]} = \alpha_s \mathcal{A}^{(1,0,0)}_{\text{EFT},gg\,[\texttt{4F}]}, \tag{2.15a}$$

$$\mathcal{A}^{(i,j,k)}_{\text{EFT},qq\,[\texttt{4F}]} = \alpha_s \mathcal{A}^{(1,0,0)}_{\text{EFT},qq\,[\texttt{4F}]} + \alpha \mathcal{A}^{(0,1,0)}_{\text{EFT},qq\,[\texttt{4F}]} + \alpha_t \mathcal{A}^{(0,0,1)}_{\text{EFT},qq\,[\texttt{4F}]}. \tag{2.15b}$$

We can then write the gg and the $q\bar{q}$-initiated interference cross-section contributions induced by the four-fermion operators in terms of all the QCD and EW coupling orders,

$$d\sigma_{\text{int},gg,[\texttt{4F}]} = \alpha_s^3\, d\sigma^{(3,0,0)}_{\text{int},gg} + \alpha_s^2 \left(\alpha\, d\sigma^{(2,1,0)}_{\text{int},gg} + \alpha_t\, d\sigma^{(2,0,1)}_{\text{int},gg} \right). \tag{2.16a}$$

$$\begin{aligned} d\sigma_{\text{int},qq,[\texttt{4F}]} = {}& \alpha_s^3\, d\sigma^{(3,0,0)}_{\text{int},qq} \\ & + \alpha_s^2 \left(\alpha\, d\sigma^{(2,1,0)}_{\text{int},qq} + \alpha_t\, d\sigma^{(2,0,1)}_{\text{int},qq} \right) \\ & + \alpha_s \left(\alpha^2\, d\sigma^{(1,2,0)}_{\text{int},qq} + \alpha^{3/2}\, \alpha_t^{1/2}\, d\sigma^{(1,3/2,1/2)}_{\text{int},qq} + \alpha\alpha_t\, d\sigma^{(1,1,1)}_{\text{int},qq} + \alpha_t^2\, d\sigma^{(1,0,2)}_{\text{int},qq} \right) \\ & + (\alpha^3)\, d\sigma^{(0,3,0)}_{\text{int},qq} + (\alpha^{5/2}\, \alpha_t^{1/2})\, d\sigma^{(0,5/2,1/2)}_{\text{int},qq} \\ & + (\alpha^2\, \alpha_t)\, d\sigma^{(0,2,1)}_{\text{int},qq} + (\alpha^{3/2}\, \alpha_t^{3/2})\, d\sigma^{(0,3/2,3/2)}_{\text{int},qq} + (\alpha\, \alpha_t^2)\, d\sigma^{(0,1,2)}_{\text{int},qq}. \end{aligned} \tag{2.16b}$$

3 Hierarchy of inclusive predictions

This section presents the numerical results from the complete LO SMEFT predictions of the $t\bar{t}t\bar{t}$ production process at $\sqrt{s} = 13$ TeV for the LHC, and at $\sqrt{s} = 100$ TeV for future circular pp colliders. The computations were performed via `MadGraph5_aMC@NLO` [19, 42] with the use of the `SMEFTatNLO` model [22], and with the mass of the top quark, m_t, set to 172 GeV. Since `MadGraph5_aMC@NLO` does not evolve the operator coefficients, and as recommended, the factorisation (μ_F), renormalization (μ_R) scales are fixed to 340 GeV$\sim (4m_t)/2$.[2] The proton PDFs and their uncertainties are evaluated employing reference sets and error replicas from the `NNPDF3.1 NLO` global fit [43] in the five flavour scheme (5FS), in which the bottom quark is taken to be massless. Unless otherwise explicitly mentioned, no parton-level cuts are imposed. Before discussing the SMEFT results, we first show the decomposition of the four-top SM cross-sections in table 1.

The strengths of the linear interference of all the dimension-six SMEFT operators belonging to the four-fermion, two-fermion, and purely-bosonic classes are presented. The interference strength is the interference cross-section in fb with the corresponding WC individually set to unity, and the scale of new physics Λ is fixed to 1(3) TeV, for the $\sqrt{s} = 13(100)$ TeV scenario. In presenting the results, the four-fermion operators are categorised into two sub-classes; contact terms involving four heavy quarks (4-heavy) and contact terms involving two heavy and two light quarks (2-heavy-2-light). Respectively, those insertions are depicted by the blobs shown in the *left* and *right* diagrams of figure 3.

[2] The EFT renormalisation scale (`mueft`) parameter of the `SMEFTatNLO` in `MadGraph5_aMC@NLO` is not relevant unless the running of the EFT coefficients is included. We do not consider the running of the EFT coefficients in this work.

$\sqrt{s}$	$\mathscr{O}(\alpha_s^4)$	$\mathscr{O}(\alpha_s^3\alpha)$	$\mathscr{O}(\alpha_s^3\alpha_t)$	$\sum_{n,m}\mathscr{O}(\alpha_s^2\alpha^n\alpha_t^m)$	$\sum_{n,m}\mathscr{O}(\alpha_s\alpha^n\alpha_t^m)$	$\sum_{n,m}\mathscr{O}(\alpha^n\alpha_t^m)$	Inclusive
13 TeV	6.15	-1.44	-0.58	2.33	$\times$	$\times$	6.46
100 TeV	2570	-313	-197	753	$\times$	$\times$	2812

Table 1. Entries in each column correspond to the LO $t\bar{t}t\bar{t}$ SM cross-section [fb] in line of α_s order, at the LHC ($\sqrt{s} = 13$) and FCC-hh ($\sqrt{s} = 100$). For contributions at $\mathscr{O}(\alpha_s^N)$ with $N = 0 - 2$, we sum all possible weak and Yukawa coupling combinations and present the total cross-section at a given order in α_s. The notation "$\times$" denotes negligible contributions. The column titled "Inclusive" shows the total cross-section.

On the other hand, since not all the two-fermion and purely-bosonic operators are relevant to $t\bar{t}t\bar{t}$ production, only the *contributing* operators from these classes are presented;

$$\{\mathcal{O}_{t\varphi}, \mathcal{O}_{tZ}, \mathcal{O}_{tW}, \mathcal{O}_{tG}, \mathcal{O}_{\varphi Q}^{(-)}, \mathcal{O}_{\varphi t}, \mathcal{O}_{G}, \mathcal{O}_{\varphi G}\}. \tag{3.1}$$

The total inclusive interference cross-section in the four-fermion case can be defined as follows:

$$\sigma_{\text{incl.}} = \sigma_3 + \sigma_2 + \sigma_1 + \sigma_0, \tag{3.2}$$

where σ_i with $i = 3, 2, 1, 0$ denotes the contributions to $\sigma_{\text{incl.}}$ arising from terms with order α_s^i in the cross-section expansion. For example, the σ_2 term denotes the interference cross-section arising *only* from the formally subleading terms in α_s, i.e. $\mathscr{O}(\alpha_s^2\alpha)$ and $\mathscr{O}(\alpha_s^2\alpha_t)$ in eq. (2.16a) and eq. (2.16b), which can be collectively written as follows:

$$\sigma_2 \equiv \alpha_s^2 \left(\alpha\, \sigma_{\text{int}}^{(2,1,0)} + \alpha_t\, \sigma_{\text{int}}^{(2,0,1)} \right). \tag{3.3}$$

The interference strength is depicted in the heat maps presented in figure 4–9, the columns correspond to the operators' coefficients. The top row shows the total inclusive interference cross-section σ_{incl} labelled `INCL`, while subsequent rows correspond to the separate contributions arranged in order of α_s, in line with the example of eq. (3.3).

$\mathbf{\sqrt{s} = 13}$ **TeV.** Starting with the 4-heavy operators in figure 4, we observe that for *all* of them, the dominant interference is the one arising from formally subleading orders, σ_2. This observation contrasts the "naive" expectation that leading (purely QCD-induced) terms would provide the highest contribution to the cross-section through σ_3 and consequently highlights the significance of the EW $tt \to tt$ scattering present in $t\bar{t}t\bar{t}$ production at LO (see figure 2). The significance of such EW scattering in four-top production has been pointed out in the NLO SM computation of ref. [2]. It is worth noting that such naive expectation not only underestimates the interference strength of the 4-heavy operators but also generates the 'wrong' sign of the interference structure. That is, σ_2 for all the 4-heavy operators has the opposite sign of σ_3. The former dictates the overall sign of the inclusive predictions. Furthermore, the lower-order-α_s cross-sections, i.e. σ_n where $n < 2$, are heavily suppressed, rendering the consideration of cross-section contributions only down to σ_2 enough to attain reliable predictions for this set of operators. Finally, for the 4-heavy operators, the colour-singlets, i.e. $\mathcal{O}_{QQ}^1$, $\mathcal{O}_{Qt}^1$, and $\mathcal{O}_{tt}^1$, are observed to have a